Progress In Electromagnetics Research C, Vol. 84, 75–85, 2018

An 8-Element Frequency-Agile MIMO Communication Antenna System for CR Front-End Applications

Sharjeel Riaz* **and Xiongwen Zhao**

Abstract—This paper presents a planar, compact 8-element frequency-reconfigurable multiple-input-multiple-output (MIMO) antenna system. The proposed design can be utilized as a communication antenna for cognitive radio (CR) front-end applications. The proposed antenna design contains 8 elements on a single substrate board. Frequency reconfigurability is achieved using varactor diode in the middle of each antenna element by varying the capacitive reactance of the slot. The proposed antenna system provides very wide frequency tunable characteristics from 1.6 to 2.48 GHz. The proposed design covers several well-known frequency bands like LTE, GSM-1800, PCS-1900, WLAN along with several others. Moreover, rectangular defected ground slots are used between vertically placed antenna elements to enhance the isolation. The complete antenna system is realized on single FR-4 substrate of dimensions $120 \times 60 \times 0.8\,\text{mm}^3$. The performance of proposed design is demonstrated by presenting both the simulated and measured results with close agreement achieved between the two which validates the proposed design.

1. INTRODUCTION

In recent years, due to exponential growth of wireless communication applications, such as GSM, LTE, UMTS, 3G, WiFi, WiMax, WLAN, ZigBee, and Bluetooth, the demand for higher data rate has increased. These demanded features require better spectrum utilization. However, it is generally recognized that spectrum remains idle for 90% of the time [1]. The spectrum congestion leads to increase in the cost of spectrum licensing, which eventually results in higher cost per bit for each user. One of the possible solutions to overcome this challenge is the implementation of cognitive radio (CR). A CR system employs frequency-reconfigurable antennas for communication at some unused frequency. A frequency-reconfigurable antenna can tune its operating band based on spectrum availability and adjust itself to dynamic environment and hence efficiently utilizes the available spectrum and addresses the spectrum crowdedness problem [1].

The RF front end of a CR system includes two types of antennas [2], an ultra-wideband (UWB) antenna for spectrum sensing and a frequency-reconfigurable antenna for multiple communications. The UWB antenna continuously monitors the wireless channel to identify unused frequency bands while the frequency-reconfigurable antenna dynamically tunes its operating frequency to communicate within the unused frequency bands. Although both these antennas are equally important, designing a frequency-reconfigurable communication antenna that is compact with switchable multiband capabilities through wide frequency range is more challenging. Slot antennas are attractive candidates for frequency reconfigurable systems due to their low cost, low profile structure, fabrication simplicity and compatibility in integration with different reconfiguration mechanisms. Many frequency reconfigurable

Received 17 March 2018, Accepted 29 April 2018, Scheduled 16 May 2018

* Corresponding author: Sharjeel Riaz (sharjeelrz85@126.com).

The authors are with the School of Electrical and Electronic Engineering, North China Electric Power University, Beijing 102206, China.

antennas with slots in their structures have appeared in literature [3–9]. Most of these designs used pin diode for frequency reconfiguration and had distinct operating frequency band.

Frequency-reconfigurable MIMO antenna systems are an appropriate choice to meet high data rate requirements for future wireless technologies because of their flexibility to operate in MIMO mode while reconfiguring their operating frequency according to system demands. Several frequency-reconfigurable MIMO antenna designs have been reported in literature [10–16]. Two-element frequency-reconfigurable MIMO antenna designs for CR applications were proposed in [10–12]. In [13], a MIMO antenna was integrated with UWB sensing antenna on the same substrate. MIMO antenna system covered frequency bands from 580 to 680 MHz and 834 to 1120 MHz. Four-element frequency-reconfigurable MIMO antenna designs were presented in [14, 15]. A frequency-reconfigurable MIMO system for CR applications covering frequency band below 1 GHz was presented in [14]. In [15], a frequency-reconfigurable MIMO slot antenna was proposed for WLAN applications covering frequency band from 2.4 to 2.5 GHz and 4.9 to 5.72 GHz. The total dimensions of the antenna were $46 \times 20 \times 1.6\,\text{mm}^3$. A two-port reconfigurable MIMO antenna with full metal rimmed design was proposed for smartphone applications in [16]. It employed a U-shaped feeding line to obtain four resonant frequencies. The frequency-reconfigurable MIMO systems cited in literature were either two-element or four-element designs.

Increasing the number of antenna elements increases the data rate and channel capacity and thus enhances the overall system performance. 8-element MIMO antenna systems that were found not frequency-reconfigurable were reported in literature [17, 18]. A MIMO antenna system for 5 GHz band with total size of $100 \times 50 \times 0.8\,\text{mm}^3$ was presented in [17]. In [18], a PIFA based MIMO system was designed covering three frequency bands: 1.88 to 1.92 GHz, 2.3 to 2.4 GHz and 2.54 to 2.62 GHz. The total substrate size was $136 \times 68.8 \times 1\,\text{mm}^3$.

In this paper, we propose an 8-element frequency-reconfigurable MIMO antenna system on a single substrate board that is suitable for wireless handheld devices in CR applications. To our knowledge, this is the first time that an 8-element frequency-reconfigurable MIMO antenna system is proposed for CR applications. The proposed design is highly compact and is confined within a board volume of $120 \times 60 \times 0.8\,\text{mm}^3$. Another distinctive feature of the proposed design is its planar structure with wide frequency tunable range from 1.6 to 2.48 GHz using varactor diode tuning. Moreover, isolation between closely spaced antenna elements is improved by using rectangular defected ground slots (DGS).

In the following sections, design details of the proposed antenna system are described in Section 2, and the simulated and measured results are discussed in Section 3. Conclusions are provided in Section 4.

2. ANTENNA SYSTEM DESIGN

Figure 1 shows our proposed 8-element frequency-reconfigurable MIMO antenna system along with biasing circuitry for varactor diodes. The fabricated model is shown in Fig. 2. The antenna system was fabricated on an FR-4 substrate with relative permittivity of 4.4 and thickness $t = 0.8\,\text{mm}$. The board contains 8 antenna elements with varactor diode in the middle of every element for frequency tuning, and rectangular DGS, which consisted of ground slots, was introduced between vertically placed antenna elements for isolation enhancement as shown in Fig. 1(b). DGS slots acted as band rejection filter and thus improved the isolation. The bottom layer has GND plane. The dimensions of the single antenna element were $22 \times 15.45\,\text{mm}^2$, and GND plane dimensions were $120 \times 60\,\text{mm}^2$. Frequency reconfigurability was achieved by variable capacitive loading effect using varactor diodes. Varactor diode was reversed biased by applying a voltage of 0 to 15 volts. Varactor diodes were utilized in all eight antenna elements to reactively load all the antenna elements. Varactor diodes used in all antenna elements were designated as D_1, D_2, D_3, D_4, D_5, D_6, D_7 and D_8.

2.1. Design of Single Antenna Element

The proposed design was started with a single rectangular slot antenna fed with $50\,\Omega$ microstrip line. The rectangular slot was selected because of inherit characteristics of rectangular slot antenna structure i.e., good input impedance matching, capability to accommodate more antenna elements with improved isolation, wide tuning range and compact antenna design. The antenna with the current dimensions

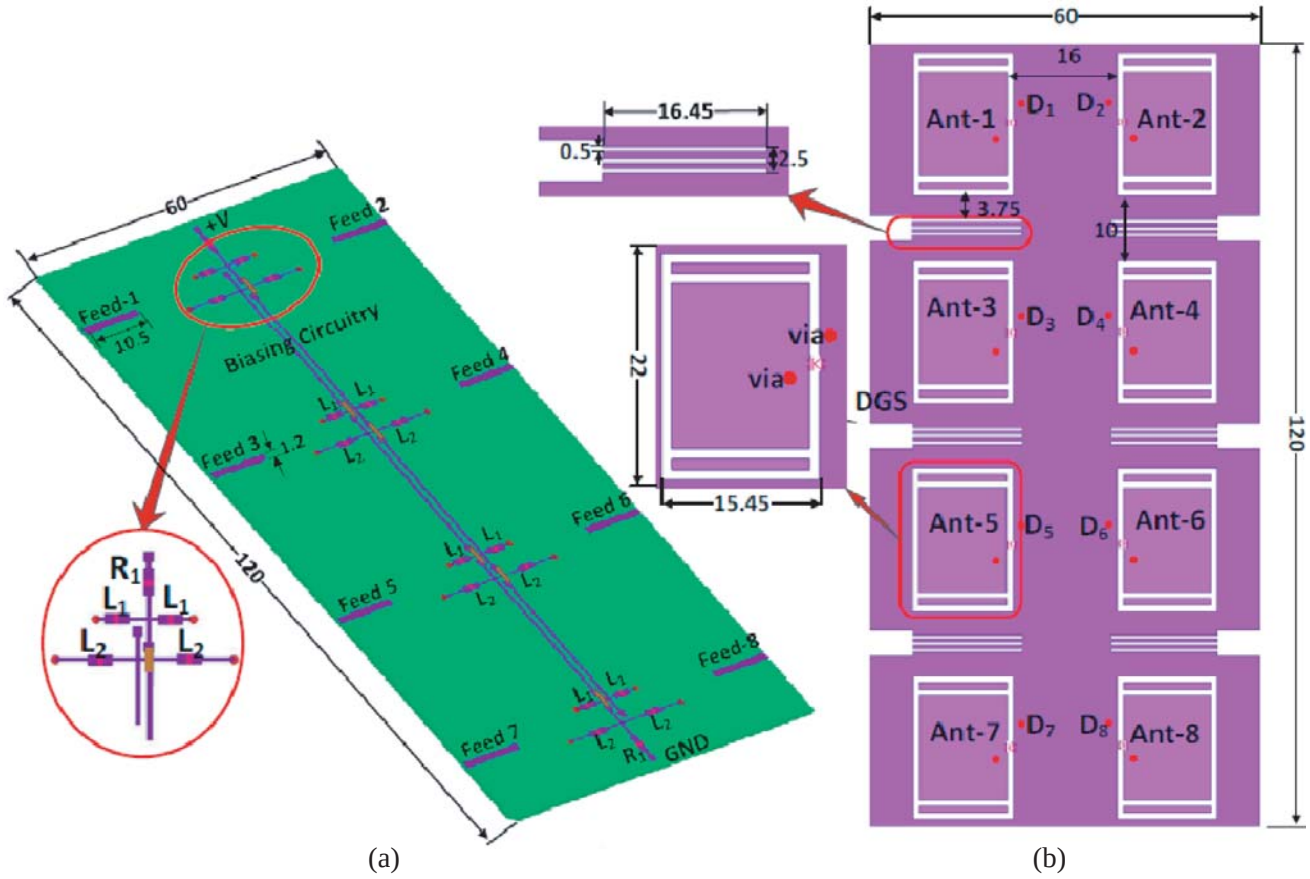

Figure 1. Proposed slot frequency-reconfigurable MIMO antenna system: (a) Top layer. (b) GND plane. All dimensions in millimeter (mm).

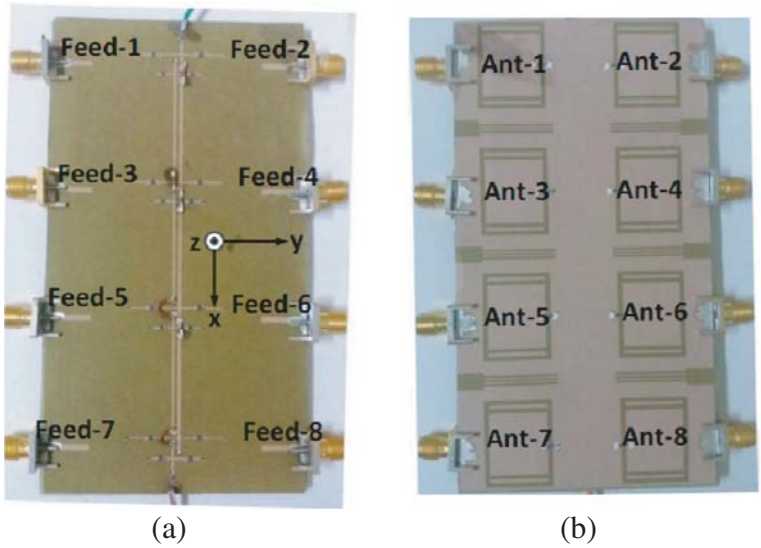

Figure 2. Fabricated eight-element frequency reconfigurable MIMO antenna system: (a) Top view. (b) Front view.

resonated at 3 GHz without any capacitive reactance. The antenna was tuned at 2.34 GHz. Parametric sweep was performed to obtain the optimal antenna element of dimensions $22 \times 15.45\,\text{mm}^2$ fed with 50-Ω microstrip line as shown in Fig. 1(b). Parametric sweeps were also used to properly place the varactor diodes to effectively load the slot. The varactor diode was on the bottom layer and connected to a biasing circuit using vias. The two additional slots were created near the shorter side of rectangle to bring down the resonance frequency to 2.31 GHz. The dimensions of the slot determine the resonance frequency of the antenna. In the proposed design, an electrical length of $\lambda/2$, corresponding to 2.31 GHz resonance band without any reactive loading, was selected. The varactor diodes were added to reactively load the rectangular slot to bring down the resonance frequency further. The varactor diodes were utilized to match the input impedance of the antenna to 50 Ω at lower frequency band around 2 GHz to cover the maximum wireless standards. For the given diode type, the maximum frequency coverage was from 1.6 GHz to 2.48 GHz.

Frequency reconfigurability was achieved by loading the rectangular slot with variable capacitance using varactor diode labeled as D_1. Varactor diode was reversed biased by applying a voltage of 0 to 15 volts. Varactor diode was on the ground plane, and the two terminals of the varactor diode were soldered across the slot, making its connection with GND plane and connecting with the biasing circuitry using two vias on the other side of the board.

2.2. Biasing Circuitry

The biasing circuitry for the proposed design is on the top layer of the board as shown in Fig. 1(a) while the schematic diagram for single varactor diode biasing is shown in Fig. 3. The varactor diode was reversed biased using variable voltage source and hence various capacitive values were obtained. Different capacitance values obtained helped in getting various resonance frequencies. The circuit consists of a series combination of an RF choke of 1 µH (L_1 and L_2) and 2.1 kΩ resistors (R_1 and R_2) connected to the two terminals of the varactor diode. The RF choke effectively blocked the AC current from power supply while the varactor diode blocked the DC current from radiating structure. The varactor diodes used were SMV 1233.

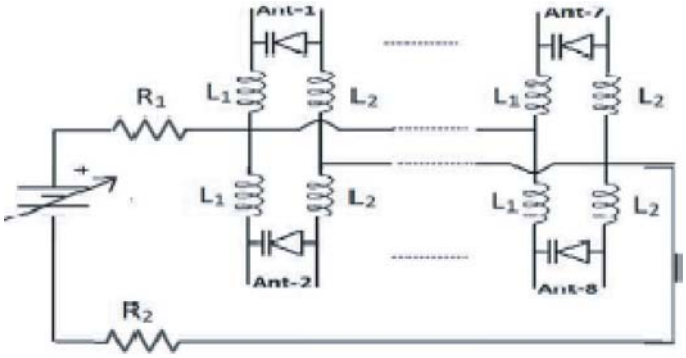

Figure 3. Varactor diode biasing circuitry.

3. RESULTS AND DISCUSSION

The proposed 8-element frequency-reconfigurable MIMO antenna was fabricated and measured. The simulations were carried out using the full-wave electromagnetic High Frequency Structure Simulator (HFSS). Measurements of S-parameters curves were obtained using Agilent Vector Network Analyzer while radiation pattern measurements were performed using SATIMO Starlab anechoic chamber.

3.1. *S*-Parameters

Figure 4(a) shows the simulated reflection coefficients curves (s_{11}) of the proposed MIMO antenna system. As all the antenna elements are similar in structure, we obtained similar results from all the

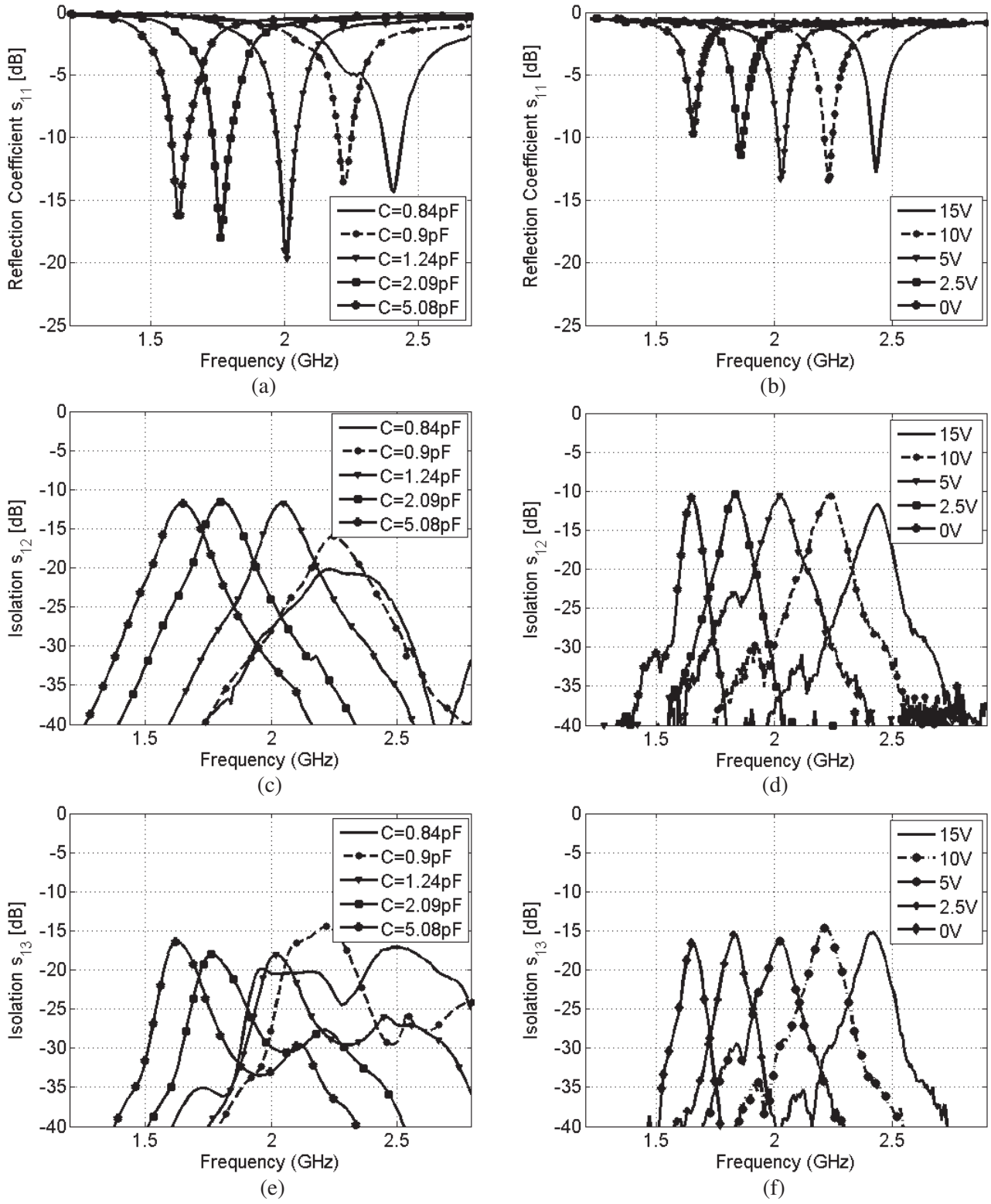

Figure 4. S-parameters: (a) Simulated S_{11}. (b) Measured S_{11}. (c) Simulated S_{12}. (d) Measured S_{12}. (e) Simulated S_{13}. (f) Measured S_{13}.

ports. Hence, the given (S_{11}) results are sufficient to give the overall picture of resonance frequency bands. The proposed design covers frequency band from 1.6 to 2.48 GHz with minimum −6 dB bandwidth of 56 MHz for each band. Fig. 4(b) shows the measured S_{11} curves of the proposed design. The smooth variation in resonating frequencies was achieved by applying reverse biased voltage to varactor diode from 0 to 15 V. These voltages correspond to different capacitance values of varactor diode. The measured operating band was from 1.6 to 2.49 GHz with −6 dB bandwidth of 61 MHz. The measured and simulated results are in good agreement. A little discrepancy in frequency can be attributed to several reasons. The substrate properties, fabrication tolerances and improper modeling of varactor diode as a variable capacitor in HFSS can be possible causes.

The proposed design was also investigated for isolation values between different antenna's ports. The simulated and measured isolation curves for the proposed eight-element frequency-reconfigurable MIMO antenna system were analyzed. The closely spaced antenna elements did not perform well without DGS structure while the isolation was greatly enhanced using the DGS structure. The simulated and measured isolation curves between different antenna elements (Ant-1, Ant-2) and (Ant-1, Ant-3) were computed. Figs. 4(c) and 4(d) show the simulated and measured curves between antenna elements Ant-1 and Ant-2, respectively, while Figs. 4(e) and 4(f) show the isolation curves for Ant-1 and Ant-3. The worst-case isolation was −12 dB between antenna elements A-1 and A-2 for simulated case and −11 dB for measured case. We have obtained similar curves for S_{23}, S_{24} and so on due to symmetrical placing of all antenna elements; therefore, they are not included. The minimum isolation values obtained for S_{13} and S_{14} were 15 dB and 16 dB, respectively, in the entire band of operation. The worst-case isolation was −8.8 dB before introducing the DGS structure while it improved to −11 dB with DGS. Hence an improvement of −2.2 dB was observed.

3.2. Current Distribution

The current distribution can be used to understand the isolation mechanism and significance of DGS in the proposed design. For the proposed MIMO slot antenna design, the worst-case isolation was observed at 1.65 GHz. Figs. 5(a) and 5(b) show the surface current density obtained at 1.65 GHz without and with DGS structure, respectively. The current distribution was obtained for Ant-2 while all other ports were terminated with 50-Ω impedance. It is evident from the figure that without DGS, there was considerable

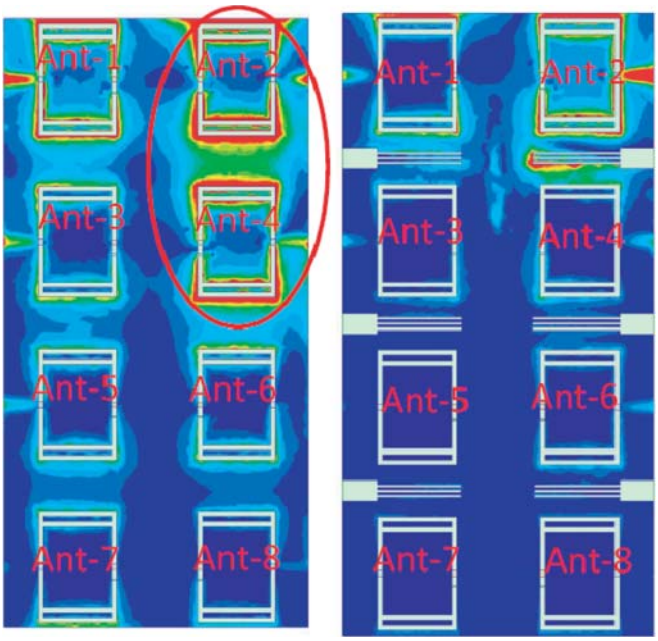

(a) (b)

Figure 5. Current density distribution at 1.65 GHz. (a) Without DGS slots. (b) With DGS slots.

coupling between Ant-2 and Ant-4, positioned side by side. This is because all antenna elements share the same GND plane. The isolation between Ant-2 and Ant-1 was acceptable with no significant coupling as the input ports are at considerable distance. The mutual coupling was significantly improved with the introduction of DGS slots between Ant-2 and Ant-4 and for other antenna elements placed side by side. The DGS structure and its locations was critical in enhancing the isolation between closely spaced antenna elements. Hence, DGS structure performed as band-stop filter at the desired frequency band and helped in minimizing the mutual coupling between closely spaced antenna elements.

3.3. Radiation Patterns and Efficiency

The gain pattern measurements were performed for single antenna element while the rest of the ports were terminated with 50 Ω loads. 3-D gain pattern of the proposed design for Ant-1 through Ant-4 is shown in Fig. 6. The peak observed was 3.88 dBi.

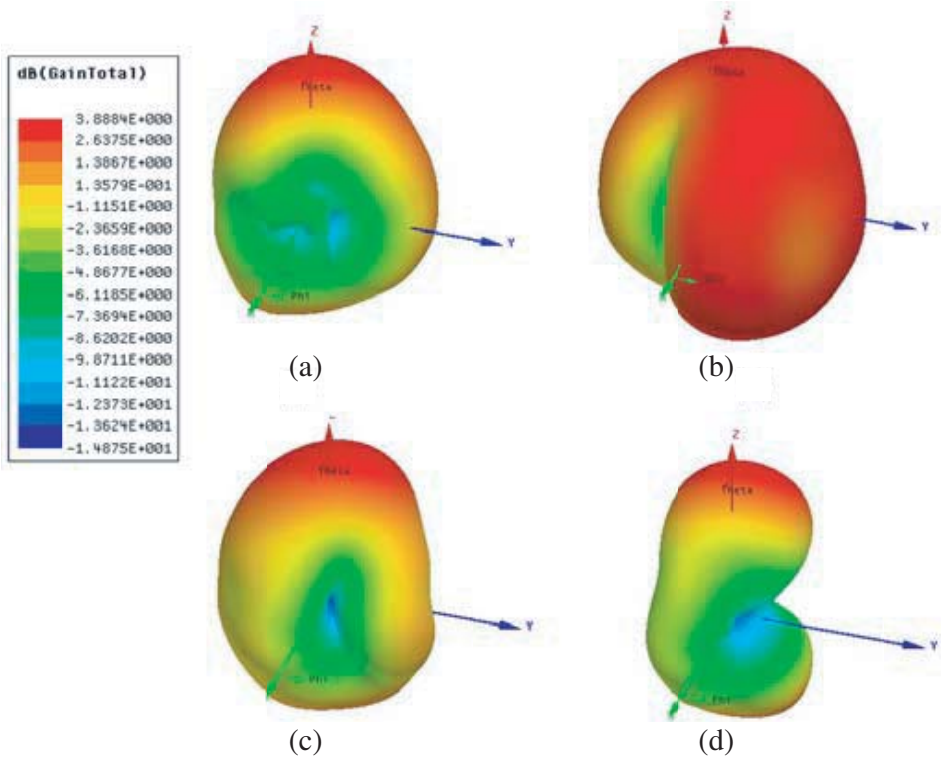

Figure 6. Simulated 3-D gain patterns at 2.41 GHz. (a) Ant-1. (b) Ant-2. (c) Ant-3. (d) Ant-4.

The simulated and measured normalized 2-D gain patterns for antennas Ant 1–4 at 2 GHz are given in Fig. 7. The patterns show the x-y and y-z planes for all the antenna elements. The simulated and measured θ-cut curves for $\phi = 0$ at 2 GHz are shown in Figs. 7(a), 7(c), while the ϕ-cut curves for $\theta = 90$ are shown in Figs. 7(b), 7(d). The gain pattern measurement setup is shown in Fig. 8.

The peak gain values and efficiency values were also obtained from measurements. A comparison between simulated and measured peak gains and efficiencies are provided in Table 1 for five simulated frequencies (f_s) and measured frequencies (f_m). Good agreement between simulated and measured values was observed.

3.4. ECC and TARC

The envelope correlation coefficient (ECC) is a measure of correlation between various communication channels. ECC values were computed using the radiation patterns in an isotropic multi-path environment. ECC values should be less than 0.5 [19]. For the given MIMO antenna system, ECC

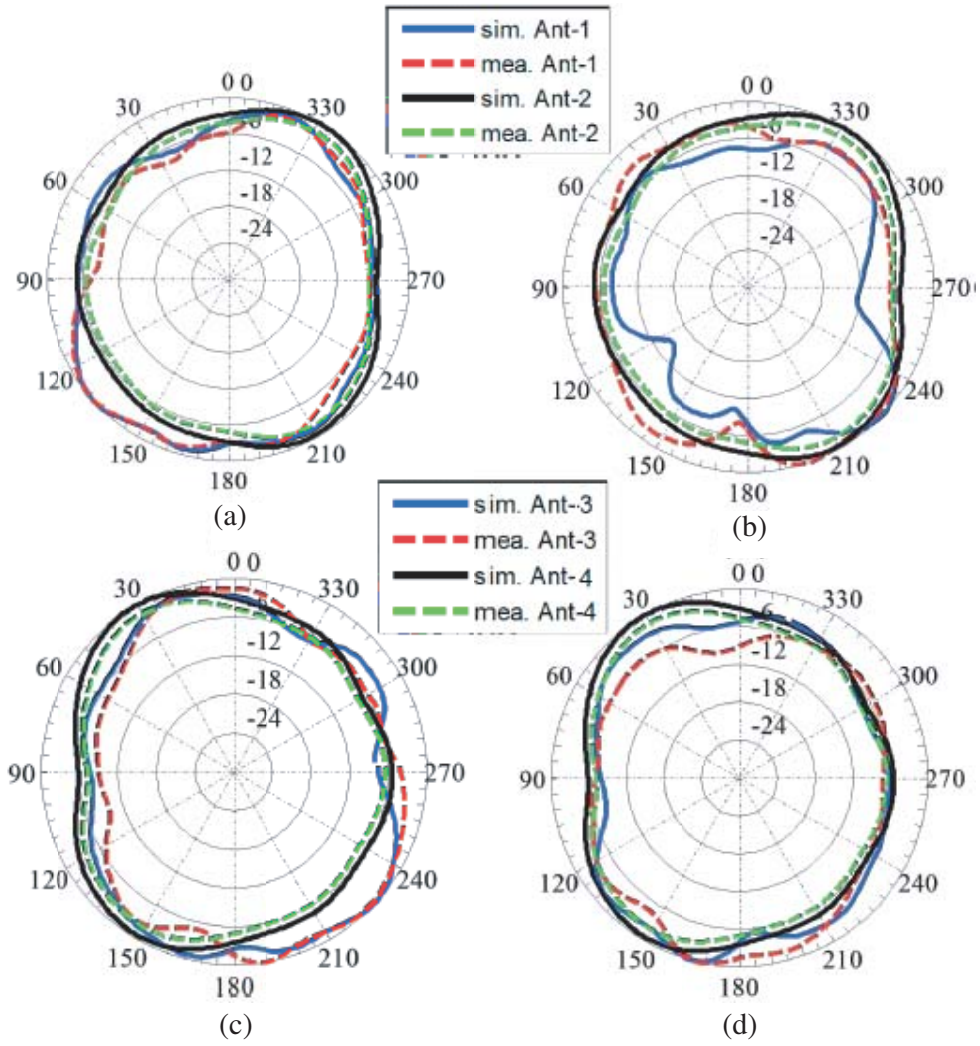

Figure 7. Measured and simulated normalized radiation pattern at 2 GHz (E_{total}). (a) (θ-cuts) Ant-1 and Ant-2 at $\phi = 0°$. (b) (ϕ-cuts) Ant-1 and Ant-2 at $\theta = 90°$. (c) (θ-cuts) Ant-3 and Ant-4 at $\phi = 0°$. (d) (ϕ-cuts) Ant-3 and Ant-4 at $\theta = 90°$.

Table 1. Efficiency and peak gain of MIMO antenna system.

Frequency (GHz)	Peak Gain (dBi)		Efficiency (%)	
	Simulated	Measured	Simulated	Measured
$f_s = 2.41,\ f_m = 2.45$	3.88	3.5	89	85
$f_s = 2.22,\ f_m = 2.10$	3.25	3.1	86	81
$f_s = 2.0,\ f_m = 2.02$	3.1	2.85	85	75
$f_s = 1.76,\ f_m = 1.79$	2.95	2.74	81	74
$f_s = 1.61,\ f_m = 1.62$	2.1	1.7	76	67

was calculated for different frequencies as given in Table 2. The given MIMO antenna system satisfies the ECC < 0.5 criterion, and hence good MIMO operation was obtained.

Total active reflection coefficient (TARC) curves for the proposed eight-element MIMO antenna system are shown in Fig. 9. Here, we have considered five cases, Case-A, Case-B, Case-C, Case-D, Case-

Figure 8. Radiation pattern measurement setup.

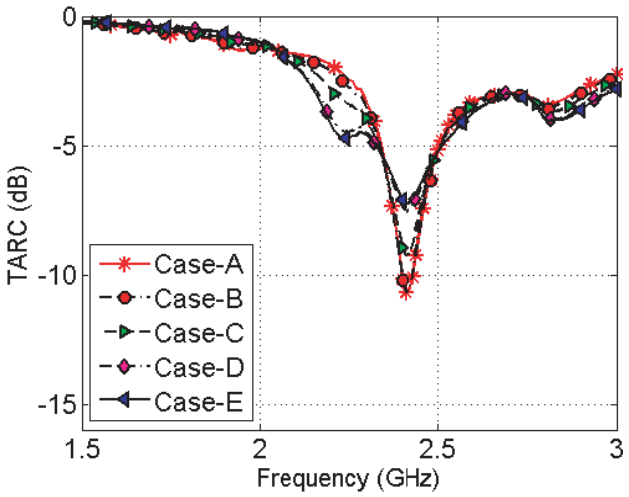

Figure 9. TARC curves at 2.41 GHz (C = 0.84 pF).

Table 2. ECC values for MIMO antenna elements.

Freq (GHz)	ECC_{12}	ECC_{13}	ECC_{14}	ECC_{15}	ECC_{16}	ECC_{17}	ECC_{18}
1.61	0.096	0.0933	0.2518	0.064	0.0246	0.064	0.0892
1.76	0.0124	0.0325	0.0125	0.0165	0.0348	0.0124	0.0239
2.0	0.0306	0.1250	0.0123	0.0124	0.0341	0.0206	0.0247
2.22	0.026	0.0783	0.0484	0.0574	0.0341	0.0267	0.0347
2.41	0.024	0.0453	0.0251	0.0681	0.0145	0.0238	0.0234

E, and corresponding excitation phases at the input ports were (0°, 30°, 45°, 60°, 90°, 120°, 150°, 180°), (0°, 30°, 45°, 45°, 60°, 60°, 90°, 90°), (0°, 30°, 60°, 45°, 30°, 90°, 120°, 150°), (0°, 60°, 45°, 30°, 30°, 150°, 150°, 180°) and (0°, 30°, 30°, 60°, 60°, 90°, 90°, 120°), respectively. In the TARC calculations, we kept phase of Port-1 equal to zero while varying the phases of other input ports. The phases of the other ports were not the same (to show the broad effect in general). TARC curves for capacitance values of 0.84 pF corresponding to 15 V are shown in Fig. 9. Although with different phase excitations, there is a slight variation in resonance curves, overall the operating bandwidth of the proposed MIMO antenna system is quite robust and not severely affected by phase changes in the excitation of the other ports. A minimum bandwidth achieved was 56 MHz for all the phases. Thus, the proposed MIMO antenna achieves a good diversity performance over the entire tuning range by satisfying the TARC criterion for MIMO antenna system.

3.5. State-of-the-Art-Comparison

There are variety of shapes available for slot antennas. Slot shape is the main parameter which affects the size of the antenna. It also affects the electrical characteristics such as polarization and gain. Table 3 compares the proposed slot antenna with recently published slot antenna designs. Most of the frequency reconfigurable slot designs reported in literature are single element antennas and only a few MIMO slot antennas. Moreover, most designs use pin diode for frequency reconfigurability and operate at some distinct frequency bands. Table 3 compares parameters such as antenna geometry, total antenna dimensions, size of the single element, number of antenna elements, achieved frequency bands, peak gain and maximum efficiency. It is evident from the table that only few designs provide

Table 3. Comparison of several frequency reconfigurable slot antenna designs.

Ref.	Slot Type	Ant. Elem.	Single Elem. Dimensions	Relative Dimensions
[3]	Rectangular	1	$30 \times 70\,\text{mm}^2$	$0.26\lambda_g \times 0.60\lambda_g$
[4]	Rectangular	1	$26 \times 40\,\text{mm}^2$	$0.27\lambda_g \times 0.42\lambda_g$
[5]	Sickle-shaped	1	$30 \times 40\,\text{mm}^2$	$0.71\lambda_g \times 0.95\lambda_g$
[6]	Rectangular	1	$87 \times 3.2\,\text{mm}^2$	$0.99\lambda_g \times 0.04\lambda_g$
[7]	Rectangular	1	$29 \times 31.3\,\text{mm}^2$	$0.39\lambda_g \times 0.43\lambda_g$
[8]	Annular	1	$r = 10.5\,\text{mm}$	$0.18\lambda_g$
[15]	Rectangular	2	$23 \times 20\,\text{mm}^2$	$0.38\lambda_g \times 0.33\lambda_g$
[16]	U-shaped	2	$18 \times 30\,\text{mm}^2$	$0.10\lambda_g \times 0.17\lambda_g$
Prop.	Rectangular	8	$22 \times 15.45\,\text{mm}^2$	$0.25\lambda_g \times 0.17\lambda_g$
Ref.	**Substrate Size $\mathbf{L \times W \times T}$ ($\mathbf{mm^3}$)**	**Achieved Bands (GHz)**	**Max Gain (dBi)**	**Efficiency (%)**
[3]	$30 \times 70 \times 0.8$	1.227, 1.381, 1.575, 2.45	2.1, 2.2, 2.1, 2.7	-
[4]	$52.8 \times 62 \times 1.6$	1.5, 1.6, 1.8, 1.9, 2.4	1.7, 2.2, 2.5, 1.75, 1.2	68, 72, 78, 76, 60
[5]	$30 \times 40 \times 1.6$	3.4–3.8, 3.7–4.2	2.21, 2.53	-
[6]	$304 \times 130 \times 1.52$	1.82, 1.93, 2.10	5.7, 5.6, 6	85, 86, 87
[7]	$80 \times 60 \times 3.04$	2.19, 2.35, 2.55, 3.1, 3.25, 3.5	3.1, 3.67, 3.76, 5.28, 6.18, 7.35	-
[8]	$32 \times 35 \times 1.6$	2.5–3.22, 4.36–6.58, 6.6–8	3.3–3.93, 2.7–4.2, 3.4–4.25	82, 88, 80
[15]	$46 \times 20 \times 1.6$	2.4, 5, 5.5	0.05, 2.9, 2.44	41, 83, 65
[16]	$145 \times 72 \times 0.8$	(0.824–0.855, 0.851–0.894, 0.878–0.920, 0.919–0.960), (1.710–2.188, 2.150–2.690)	0.32–1.4, 1.6–4.8	43, 59–72
Prop.	$120 \times 60 \times 0.8$	1.6 to 2.5 (continuous tuning)	1.7, 2.74, 2.85, 3.1, 3.5	67, 74, 75, 81, 85

The letters L, W, T denote length, width and thickness.

continuous tuning range. The proposed design exhibits a wide range tunability (1.6 to 2.48 GHz) for this frequency range, has very good performance with respect to antenna size, gain, efficiency, and can accommodate eight elements in a limited ground size. Therefore, the proposed design is well suited for future wireless communications and cognitive radio applications.

4. CONCLUSION

A novel 8-element frequency-reconfigurable MIMO antenna system covering frequency band from 1.6 to 2.48 GHz is presented in this paper. The proposed design having a planar structure and compact size ($120 \times 60 \times 0.8\,\text{mm}^3$) is a suitable communication antenna for CR front-end applications. This 8 antenna element design was confined within a single substrate and employed varactor diodes for frequency reconfigurability. The proposed MIMO antenna system is a suitable candidate for CR applications in wireless handheld devices. The achieved results for ECC and TARC show good MIMO performance of the proposed design. Moreover, good isolation between antenna elements was achieved using rectangular DGS.

ACKNOWLEDGMENT

This work is supported by Beijing Municipal Science & Technology Commission under project entitled "Research on 5G channel modeling technologies for massive machine communications".

REFERENCES

1. Mitola, J., "Cognitive radio architecture evolution," *Proc. IEEE*, Vol. 97, No. 4, 626–641, Apr. 2009.
2. Christodoulou, C. G., "Cognitive radio: The new frontier for antenna design?," *IEEE Antennas Propag. Soc. Feature Art.*, [Online], Available: www.ieeeaps.org.
3. Hung, C. and T. Chiu, "Dual-band reconfigurable antenna design using slot-line with branch edge," *IEEE Trans. Antennas Propag.*, Vol. 63, No. 2, 508–516, Feb. 2015.
4. Sharma, S. and C. C. Tripathi, "Frequency reconfigurable U-slot antenna for SDR application," *Progress In Electromagnetics Research Letters*, Vol. 55, 129–136, 2015.
5. Han, L., C. Wang, W. Zhang, R. Ma, and Q. Zeng, "Design of frequency- and pattern-reconfigurable wideband slot antenna," *Int. J. Antennas Propag.*, Vol. 2018, Art. ID: 3678018, 1–7, 2018.
6. Majid, H. A., M. K. A. Rahim, M. R. Hamid, and M. F. Ismail, "Frequency and pattern reconfigurable slot antenna," *IEEE Trans. Antennas Propag.*, Vol. 62, No. 10, 5339–5343, Oct. 2014.
7. Majid, H. A., M. K. A. Rahim, M. R. Hamid, and M. F. Ismail, "Frequency reconfigurable microstrip patch-slot antenna with directional radiation pattern," *Progress In Electromagnetics Research*, Vol. 144, 319–328, 2014.
8. Gholamrezaei, M., F. Geran, and R. A. Sadeghzadeh, "Completely independent multi-ultrawideband and multi-dual-band frequency reconfigurable annular sector slot antenna (FR-ASSA)," *IEEE Trans. Antennas Propag.*, Vol. 65, No. 2, 893–898, Feb. 2017.
9. Sharma, S. and C. C. Tripathi, "A novel reconfigurable antenna with spectrum sensing mechanism for CR system," *Progress In Electromagnetics Research C*, Vol. 72, 187–196, 2017.
10. Tawk, Y., J. Costantine, and C. Christodoulou, "Reconfigurable filtennas and MIMO in cognitive radio applications," *IEEE Trans. Antennas Propag.*, Vol. 62, No. 3, 1074–1084, Mar. 2014.
11. Lim, J.-H., Z.-J. Jin, C.-W. Song, and T.-Y. Yun, "Simultaneous frequency and isolation reconfigurable MIMO PIFA using pin diodes," *IEEE Trans. Antennas Propag.*, Vol. 60, No. 12, 5939–5946, Dec. 2012.
12. Cao, Y., S. W. Cheung, and T. I. Yuk, "Frequency-reconfigurable multiple-input-multiple-output monopole antenna with wide-continuous tuning range," *IET Microw. Antennas Propag.*, Vol. 10, No. 12, 1322–1331, May 2016.
13. Hussain, R. and M. S. Sharawi, "A cognitive radio reconfigurable MIMO and sensing antenna system," *IEEE Antennas Wireless Propag. Lett.*, Vol. 14, 257–260, 2015.
14. Hussain, R. and M. S. Sharawi, "Planar meandered-F-shaped 4-element reconfigurable multiple-input-multiple-output antenna system with isolation enhancement for cognitive radio platforms," *IET Microw. Antennas Propag.*, Vol. 10, No. 1, 45–52, Sep. 2015.
15. Soltani, S., P. Lotfi, and R. D. Murch, "A port and frequency reconfigurable MIMO slot antenna for WLAN applications," *IEEE Trans. Antennas Propag.*, Vol. 64, No. 4, 1209–1217, Apr. 2016.
16. Xu, Z. Q., Y. T. Sun, Q. Q. Zhou, Y. L. Ban, Y. X. Li, and S. S. Ang, "Reconfigurable MIMO antenna for integrated-metal-rimmed smartphone applications," *IEEE Access*, Vol. 5, 21223–21228, 2017.
17. Sharawi, M. S., "A 5-GHz 4/8-element MIMO antenna system for IEEE 802.11ac devices," *Microw. Opt. Technol. Lett.*, Vol. 55, No. 7, 1589–1594, Jul. 2013.
18. Qin, Z., W. Geyi, M. Zhang, and J. Wang, "Printed eight-element MIMO system for compact and thin 5G mobile handset," *Electron. Lett.*, Vol. 52, No. 6, 416– 418, Mar. 2016.
19. Sharawi, M. S., *Printed MIMO Antenna Engineering*, Artech House, 2014.